WIND TUNNEL STUDY OF WIND FRAME LOADS ON BROAD FINANCIAL CENTER, NEW YORK

by

J. A. Peterka,* S. T. Thoroddsenn* and
J. E. Cermak***

FLUID MECHANICS AND
WIND ENGINEERING PROGRAM

COLLEGE OF ENGINEERING

COLORADO STATE UNIVERSITY
FORT COLLINS, COLORADO

WIND TUNNEL STUDY OF WIND FRAME LOADS ON BROAD FINANCIAL CENTER, NEW YORK

by

J. A. Peterka,* S. T. Thoroddsenn* and
J. E. Cermak***

for

Fox and Fowle Architects, P.C.
192 Lexington Avenue
New York, New York 10016

Fluid Mechanics and Wind Engineering Program
Fluid Dynamics and Diffusion Laboratory
Department of Civil Engineering
Colorado State University
Fort Collins, Colorado 80523

CSU Project 2-96080

December 1984

*Professor
**Graduate Research Assistant
***Professor-in-Charge, Fluid Mechanics
and Wind Engineering Program

TABLE OF CONTENTS

LIST OF FIGURES

LIST OF TABLES

LIST OF SYMBOLS

Symbol	Definition
U	Local mean velocity
ν,ρ	Kinematic viscosity and density of approach flow
$\frac{UD}{\nu}$	Reynolds number
E	Mean voltage
U_{rms}	Root-mean-square of fluctuating velocity
E_{rms}	Root-mean-square of fluctuating voltage
U_{∞}	Reference mean velocity outside the boundary layer
X,Y	Horizontal coordinates
Z	Height above surface
δ	Height above surface of boundary layer
T_u	Turbulence intensity $\frac{U_{rms}}{U_{\infty}}$ or $\frac{U_{rms}}{U}$
A_R	Reference area
L_R	Reference length of building
CF_x	Force coefficient, x direction, $\frac{F_x}{A_R\ 0.5\rho\ U_{\infty}^2}$
CF_y	Force coefficient, y direction, $\frac{F_y}{A_R\ 0.5\rho\ U_{\infty}^2}$
F_x,F_y	Forces in x, y direction
M_x,M_y	Moments around x, y axes

1. INTRODUCTION

1.1 General

A significant characteristic of modern building design is lighter cladding and more flexible frames. These features produce an increased vulnerability of glass and cladding to wind damage and result in larger deflections of the building frame.

The building geometry itself may increase or decrease wind loading on the structure. Wind forces may be modified by nearby structures which can produce beneficial shielding or adverse increases in loading. Overestimating loads results in uneconomical design; underestimating may result in cladding or window failures.

Techniques have been developed for wind tunnel modeling of proposed structures which allow the prediction of wind pressures on cladding and windows, overall structural loading and also wind velocities and gusts in pedestrian areas adjacent to the building. Accurate knowledge of the wind loading for a selected maximum design wind permits economical design of the frame for flexural control.

Modeling of the aerodynamic loading on a structure requires special consideration of flow conditions in order to guarantee similitude between model and prototype. A detailed discussion of the similarity requirements and their wind-tunnel implementation can be found in references (1), (2), and (3). In general, the requirements are that the model and prototype be geometrically similar, that the approach mean velocity at the building site have a vertical profile shape similar to the full-scale flow, that the turbulence characteristics of the flows be similar, and that the Reynolds number for the model and prototype be equal.

These criteria are satisfied by constructing a scale model of the structure and its surroundings and performing the wind tests in a wind tunnel specifically designed to model atmospheric boundary-layer flows. Reynolds number similarity requires that the quantity UD/ be similar for model and prototype. Since , the kinematic viscosity of air, is identical for both, Reynolds numbers cannot be made precisely equal with reasonable wind velocities. To accomplish this the air velocity in the wind tunnel would have to be as large as the model scale factor times the prototype wind velocity, a velocity which would introduce unacceptable compressibility effects. However, for sufficiently high Reynolds numbers ($>2\times10^4$) the pressure coefficient at any location on the structure will be essentially constant for a large range of Reynolds numbers. Typical values encountered are 10^7-10^8 for the full-scale and 10^5-10^6 for the wind-tunnel model. In this range acceptable flow similarity is achieved without precise Reynolds number equality.

1.2 The Wind-Tunnel Test

The wind-engineering study is performed on a building or building group modeled at scales ranging from 1:150 to 1:500. The building model is constructed of a light weight material and then mounted on the force balance. The structure is modeled in detail to provide accurate flow patterns in the wind passing over the building surfaces. The building under test is often located in a surrounding where nearby buildings or terrain may provide beneficial shielding or adverse wind loading. To achieve similarity in wind effects the area surrounding the test building is also modeled. A flow visualization study is first made (smoke is used to make the air currents visible) to define overall flow patterns and identify regions where local flow features might cause

difficulties in building curtain-wall design or produce pedestrian discomfort.

The test model is mounted on a force balance and exposed to an appropriately modeled atmospheric wind in the wind tunnel. The fluctuating wind loading is measured electronically. The data is recorded, analyzed and processed by an on-line computerized data-acquisition system. The model and model area is rotated 360 degrees in 10 degree increments, to measure the effect of different wind directions. If thought to be necessary data is taken in smaller azimuthal steps. Using wind data applicable to the building site, representative wind velocities are selected to scale the loading.

The following pages discuss in greater detail the procedures followed and the equipment and data collecting and processing methods used. In addition, the data presentation format is explained and the implications of the data are discussed.

2. EXPERIMENTAL CONFIGURATION

2.1 Wind Tunnel

Wind-engineering studies are performed in the Fluid Dynamics and Diffusion Laboratory at Colorado State University (Figure 1). Three large wind tunnels are available for wind loading studies depending on the detailed requirements of the study. The wind tunnel used for this study was the Industrial Aerodynamics Wind Tunnel which is shown in Figure 2. All tunnels have a flexible roof adjustable in height to maintain a zero pressure gradient along the test section. The mean velocity can be adjusted continuously in each tunnel to the maximum velocity available.

2.2 Model

In order to obtain an accurate assessment of the wind loading, models are constructed to the largest scale that does not produce significant blockage in the wind-tunnel test section.

A scale of 1:500 was selected. The model was built out of solid balsa-wood, see Figure 3. A hole was drilled into the model so as to mount it on the force-balance tube.

A circular area 750 to 2000 ft in radius depending on model scale and characteristics of the surrounding buildings and terrain is modeled in detail. Structures within the modeled region are made from styrofoam and cut to the individual building geometries. They are mounted on the turntable in their proper locations. Significant terrain features are included as needed. The model is mounted on a turntable (Figure 2) near the downwind end of the test section. Any significant buildings or terrain features which did not fit on the turntable were placed on removable pieces which were placed upwind of the turntable for

appropriate wind directions. A view of the building and its surroundings is shown in Figure 4. The turntable is calibrated to indicate azimuthal orientation to 0.1 degree.

The region upstream from the modeled area is covered with a randomized roughness constructed using various sized cubes placed on the floor of the wind tunnel. Different roughness sizes may be used for different wind directions. Spires are installed at the test-section entrance to provide a thicker boundary layer than would otherwise be available. The thicker boundary layer permits a somewhat larger scale model than would otherwise be possible. The spires are approximately triangularly shaped pieces of 1/2 in. thick plywood 6 in. wide at the base and 1 in. wide at the top, extending from the floor to the top of the test section. They are placed so that the broad side intercepts the flow. A barrier approximately 8 in. high is placed on the test-section floor downstream of the spires to aid in development of the boundary-layer flow.

The distribution of the roughness cubes and the spires in the roughened area was designed to provide a boundary-layer thickness of approximately 4 ft, a velocity profile power-law exponent similar to that expected to occur in the region approaching the modeled area for each wind direction (a number of wind directions may have the same approach roughness). A photograph of the completed model in the wind tunnel is shown in Figure 5. The wind-tunnel ceiling is adjusted after placement of the model to obtain a zero pressure gradient along the test section.

2.3 Boundary Layers

Mean velocity and turbulence intensity profiles are measured upstream of the model to determine that an approach boundary-layer flow appropriate to the site has been established. Tests are made at one wind velocity in the tunnel. This velocity is well above that required to produce Reynolds number similarity between the model and the prototype as discussed in Section 1.1.

Measurements are made with a single hot-wire anemometer mounted with its axis vertical. The instrumentation used is a Thermo Systems constant temperature anemometer (Model 1050) with a 0.001 in. diameter platinum film sensing element 0.020 in. long. Output is directed to the on-line data acquisition system for analysis.

Calibratin of the hot-wire anemometer is performed by comparing output with the pitot-static tube in the wind tunnel. The calibration data are fit to a variable exponent King's Law relationship of the form

$$E^2 = A + BU^n$$

where E is the hot-wire output voltage, U the velocity and A, B, and n are coefficients selected to fit the data. The above relationship was used to determine the mean velocity at measurement points using the measured mean voltage. The fluctuating velocity in the form U_{rms} (root-mean-square velocity) was obtained from

$$U_{rms} = \frac{2\ E\ E_{rms}}{B\ n\ U^{n-1}}$$

where E_{rms} is the root-mean-square voltage output from the anemometer. Turbulence intensity in the velocity profile measurements were divided by the local mean velocity.

3. INSTRUMENTATION

3.1 Force Balance

The force balance used in this project is shown in Figure 6. Basically it is a strain-sensing apparatus consisting of three main parts: a heavy steel reaction or inertial ring, a steel sprung plate supported by steel cross-beams, and a stem of aluminum tubing. The reaction ring is bolted to the wind tunnel turntable just below the floor level. The entire balance rotates along with the model on the turntable, and thus defines a body-centered coordinate system. This right-handed coordinate system (Figure 6) is oriented with the z-axis coinciding with the model and force balance vertical axis, and the x and y axes in the horizontal plane. The height of this plane is at two different levels, defined by an upper and lower set of strain gages attached to the sprung portion of the balance. Each level has two complete strain gage bridge networks which sense the total bending moment about the x and y axes at that level, the bending moment being the result of wind forces on the entire container model. Figure 6 shows schematically the means by which the moments about the y-axis at level 1 (My_1) and level 2 (My_2) are sensed.

The strain gages at level one are attached to necked-down segments of the steel cross-members which connect the sprung portion of the balance to the reaction base. The upper gages are attached to the stem, and can be seen in Figure 3. All strain gages are p-type silicon semiconductor electrcal resistance gages, having a nominal gage factor of about 140. The lower gages are type SPB3-20-35 by BLH, and the upper gages are type BG-1-500 by Micro-Engineering II. Gage excitation and

amplification were provided by Accudata model 218 gage control/ amplifiers, manufactured by Honeywell.

The building model was built and mounted in such a waythat all loads are transmitted to the stem above level 2. This results in two important characteristics: 1) constant shear force in the stem between levels 1 and 2, proportional to the difference in moment at the two levels, and 2) a moment in the stem which varies linearly between the two levels.

The balance was designed to have a high natural frequency of vibration to permit the measurement of dynamic loading without excessive resonant amplification. But since we are only measuring the mean loading in this study, this criterion is not of importance.

Calibration of the entire force balance system was performed in the wind tunnel using the same electronics and data-acquisition system used during testing. Weights and a fish-line were used to pull on the stem at a certain position and the output was monitored at the same time. The resulting calibration curves are extremely linear as is shown in Figure 7.

The strain-gage output has a tendency to drift as the tunnel temperature changes. To minimize this drift a zero measurement was taken before and after each wind tunnel run. If an unusual drift was observed the test was repeated. Sample time was also kept as small as possible, but long enough to get a stable mean.

3.2 Data Acquisition

The analog signals from the strain gages are increased by gage amplifiers to approximate ±10 volts full scale. The signals are also filtered by low-pass filters with cut-off frequency at 100 Hz.

The reference pressure is measured by a Pitot-static tube located along the tunnel centerline at the gradient height (950 ft full-scale) (see Figure 5). The total and static pressure tubes from this sensor were routed to a differential pressure transducer, which provides an output signal proportional to the dynamic pressure $\frac{1}{2}\rho U^2$. The transducer and a dedicated gage control/amplifier are maintained and calibrated together as a unit, and produce a high-level signal precisely related to the reference pressure.

The analog to digital conversion is accomplished by a Preston Scientific 12-bit, 50 kHz, 16-channel AD. The computer software involved was developed by ERC-FDDL personnel. The main computer is an HP 1000 21MX E-series. It includes a disc drive, printer and plotter.

By scaling the data correctly we get the absolute moments at position 1 and 2 (see Figure 6). By assuming a linear variation of the moment, the moment at ground level is readily calculated. The shear is constant because all of the loading is transferred to the stem above level 2. So

$$F = \frac{M_2 - M_1}{a}$$

where "a" is the vertical distance between moment measurements. See figure B for the derivation of this equation.

4. RESULTS AND DISCUSSION

4.1 Velocity Profiles

Velocity and turbulence profiles approaching the model turntable are shown in Figures 9 and 10. Profiles were taken upstream of the turntable and are characteristic of the boundary layer approaching the building site, one over the sea and the other over the city. The boundary-layer thickness, δ, is given both in model and corresponding prototype values. This value was established as a reasonable height for this study. The mean velocity profile approaching the modeled area has the form

$$\frac{U}{U_\infty} = \left(\frac{z}{\delta}\right)^n \ .$$

The exponents n for the approch flow were established by studying the topography and structures in the vicinity. The values are given in Figures 9 and 10.

Profiles of longitudinal turbulence intensity of the approach flow are also shown in the same figures. The turbulence intensities are appropriate for the approach mean velocity profile selected. For the velocity profiles, turbulence intensity is defined as the root-mean-square about the mean of the longitudinal velocity fluctuations divided by the local mean velocity U,

$$Tu = \frac{U_{rms}}{U} \ .$$

The velocity profile for the wind coming over the sea was generated by laying pegboards (1/4" roughness) on the tunnel floor, besides using spires and a trip at the entrance, see Figure 5. The spires and the trip were also used for the velocity profile coming over the city, but in this case, 1" and 2" roughness elements were used.

Two velocity profiles at the building site were measured. The building under study was removed and the velocity profile inside the city at the proposed building site was measured. This is done to get a rough idea of the influence of the close-by buildings on the flow field. The resulting profiles are shown in Figures 11 and 12.

4.2 Forces and Moments

Moment coefficients around x and y-axes were measured at levels 1 and 2, see Figure 6. These coefficients are defined as shown below:

$$CM_x = \frac{M_x}{A_R L_R 0.5 \rho U_\infty^2}$$

and similarly for CM_y. Terms and symbols are defined in the List of Symbols. By scaling A_R and L_R up to prototype size and selecting the appropriate gradient wind speed U_∞ we can calculate the actual prototype moments acting on the building. By methods described in Chapter 2 and Figure 8 we calculate the resulting moment at ground level and the shear. The moments and shear were calculated in the building coordinate axes, shown in Figure 13. They were transformed to prototype scale using the mean one-hour 100-year recurrence wind. The results are shown in Figures 14 and 15 and Table 2.

The loads reported include wind directional load factors, which are shown in Table 1 and compensate for the fact that wind from all directions is not equally probable. Keeping this in mind the high x-moments occur for 130 and 290 degree wind and a high y-moment for 180 degree wind. The relation between wind and surroundings is shown in Figure 16 for these two cases.

The loads reported in Table 2 are hourly mean loads. The gust load factor, shown in Table 1, is used to increase the loads from an hourly

mean load to that of a gust whose duration would be sufficient for its effect to be fully felt by the structure. A table of gust load factors for various gust durations is incorporated in Table 1 so that force and moment data of Table 2 may be adjusted to different load duration if desired.

The overall forces and moments on the full-scale building due to wind loading reported herein are essential in designing the structural framing of the proposed building.

REFERENCES

1. Cermak, J. E., "Laboratory Simulation of the Atmospheric Boundary Layer," AIAA Jl., Vol. 9, September 1971.

2. Cermak, J. E., "Applications of Fluid Mechanics to Wind Engineering," A Freeman Scholar Lecture, ASME Jl. of Fluids Engineering, Vol. 97, No. 1, March 1975.

3. Cermak, J. E., "Aerodynamics of Buildings," Annual Review of Fluid Mechanics, Vol. 8, 1976, pp. 75-106.

4. American National Standards Institute, "American National Standard Building Code Requirements for Minimum Design Loads in Buildings and Other Structures," ANSI Stnadard A58.1, 1972, or the revised ANSI Standard A58.1 to be published.

5. Hollister, S. C., "The Engineering Interpretation of Weather Bureau Records for Wind Loading on Structures," Building Science Series 30--Wind Loads on Buildings and Structures, National Bureau of Standards, pp. 151-164, 1970.

6. Simiu, E. and R. H. Scanlan, Wind Effects on Structures: An Introduction to Wind Engineering, John Wiley & Sons, New York, 1978.

TABLE 1

CALCULATION OF REFERENCE VELOCITIES

1. Basic wind speed from directional wind data including the influence of hurricanes*:

Largest 100-year fastest mile at 33 ft for SE wind = 86 mph

Largest mean hourly wind speed, 33 ft = $\frac{86}{1.28}$ = 67.2 mph, see reference [6] on page 62

Mean hourly gradient wind speed = 67.2 (1.54)** = 121 mph

Réference wind speed U_∞ = wind speed at 950 ft

Wind Direction	Approach Wind Profile Power Law Exponent	Reference Pressure at 950 ft / Reference Pressure at Gradient
80°-330°	0.14	1.0
0-70°,340-350°	0.32	$(\frac{950}{1500})^{(.32)(2)}$ = 0.747

*Data on directionality based on:

Batts, M. E., M. R. Cordes, L. R. Russel, J. R. Shaver, E. Simiu, "Hurricane Wind Speeds in the United States," NBS Building Science Series 124, National Bureau of Standards, 1980.

and National Climatic Center Wind Speeds at La Guardia Airport.

**Based on hurricane data.

2. Loads including wind directionality and hurricanes--New York City.

Mean hourly gradient wind at milepost 2550.

Wind Direction	Gradient Mean Wind Speed (ws) mph	Gradient Level Load Ratio $(ws/121)^2$	Load Ratio for Reference Pressure at 950 ft
N (0°)	94	0.61	0.46
NNE	96	0.63	0.48
NE	109	0.81	0.61
ENE	119	0.97	0.73
E (90°)	114	0.89	0.89
ESE	119	0.97	0.97
SE	121	1.00	1.00
SSE	115	0.90	0.91
S (180°)	118	0.95	0.96
SSW	109	0.81	0.82
SW	94	0.60	0.61
WSW	96	0.63	0.63
W (270°)	100	0.68	0.69
WNW	108	0.80	0.80
NW	103	0.72	0.73
NNW	94	0.61	0.61

3. Gust load factors to convert hourly mean integrated load to mean load for various gust durations (see Section 4.2):

Gust Duration, (sec)	Gust Load Factor
10-15	$(1.40)^2 = 1.96$
30	$(1.32)^2 = 1.74$
45	$(1.26)^2 = 1.59$

BROAD FINACIAL CENTER, NEW YORK City environment, 100 yr return wind

UD	MX	MY	FX	FY
	1000-KIP-FT		KIP	
0	5.1	45.0	311.8	-51.6
10	5.8	52.1	372.2	-48.0
20	-3.5	10.5	125.3	-1.7
30	-6.2	16.8	149.4	18.0
40	.8	27.6	206.4	-3.3
50	6.2	54.8	362.7	-51.9
60	-5.3	38.6	277.5	3.6
70	-10.1	16.5	153.3	28.2
80	-23.3	-1.4	60.2	116.0
90	-37.4	-21.5	-125.0	221.4
100	-33.6	41.0	169.3	210.2
110	-33.7	97.0	318.0	198.3
120	-61.9	75.5	59.8	339.8
130	-76.6	55.1	-54.2	406.8
140	-74.7	18.0	-222.1	401.1
150	-63.2	-18.5	-330.0	338.0
160	-38.5	-31.3	-243.8	229.4
170	18.0	40.0	149.7	-18.8
180	40.5	125.5	517.7	-32.6
190	35.2	118.6	425.3	-20.1
200	43.5	74.7	262.4	-92.2
210	45.3	-33.9	-293.2	-100.9
220	-2.0	-46.4	-312.6	16.5
230	-17.5	-34.1	-280.4	27.8
240	-14.8	-41.3	-303.0	16.0
250	-7.2	-71.5	-446.3	-8.1
260	17.3	-111.5	-610.0	-82.3
270	45.2	-128.0	-648.7	-180.4
280	58.4	-112.2	-526.2	-226.7
290	63.6	-116.6	-548.4	-232.5
300	52.4	-59.1	-214.5	-201.7
310	32.7	-22.4	85.1	-143.4
320	31.5	-3.7	241.4	-135.4
330	22.4	22.5	283.8	-91.0
340	25.9	33.7	334.6	-120.0
350	10.8	37.0	314.0	-69.2

Table 2. Moments and Shear Forces.

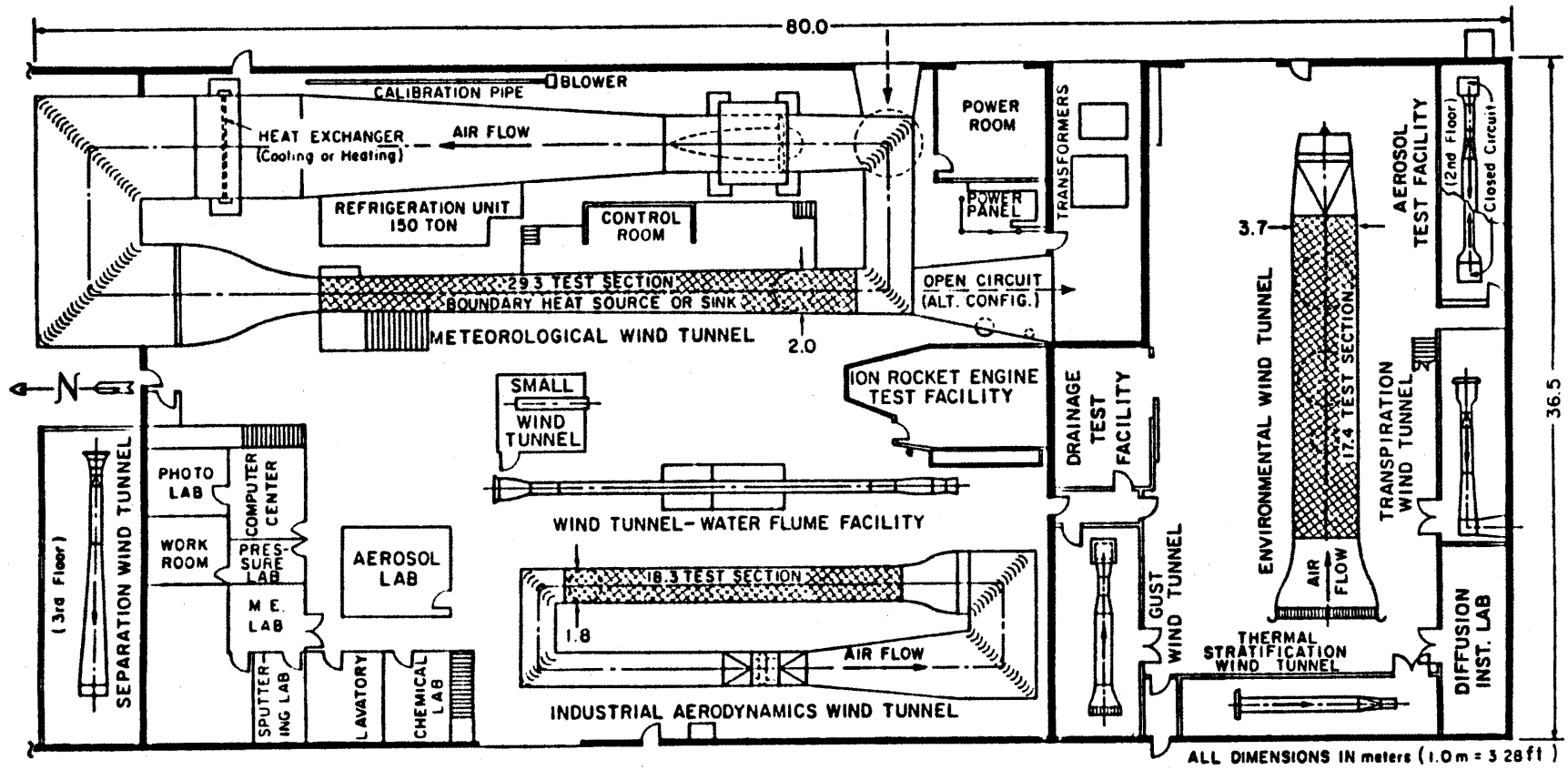

FIG. 1. FLUID DYNAMICS AND DIFFUSION LABORATORY
ENGINEERING RESEARCH CENTER
COLORADO STATE UNIVERSITY

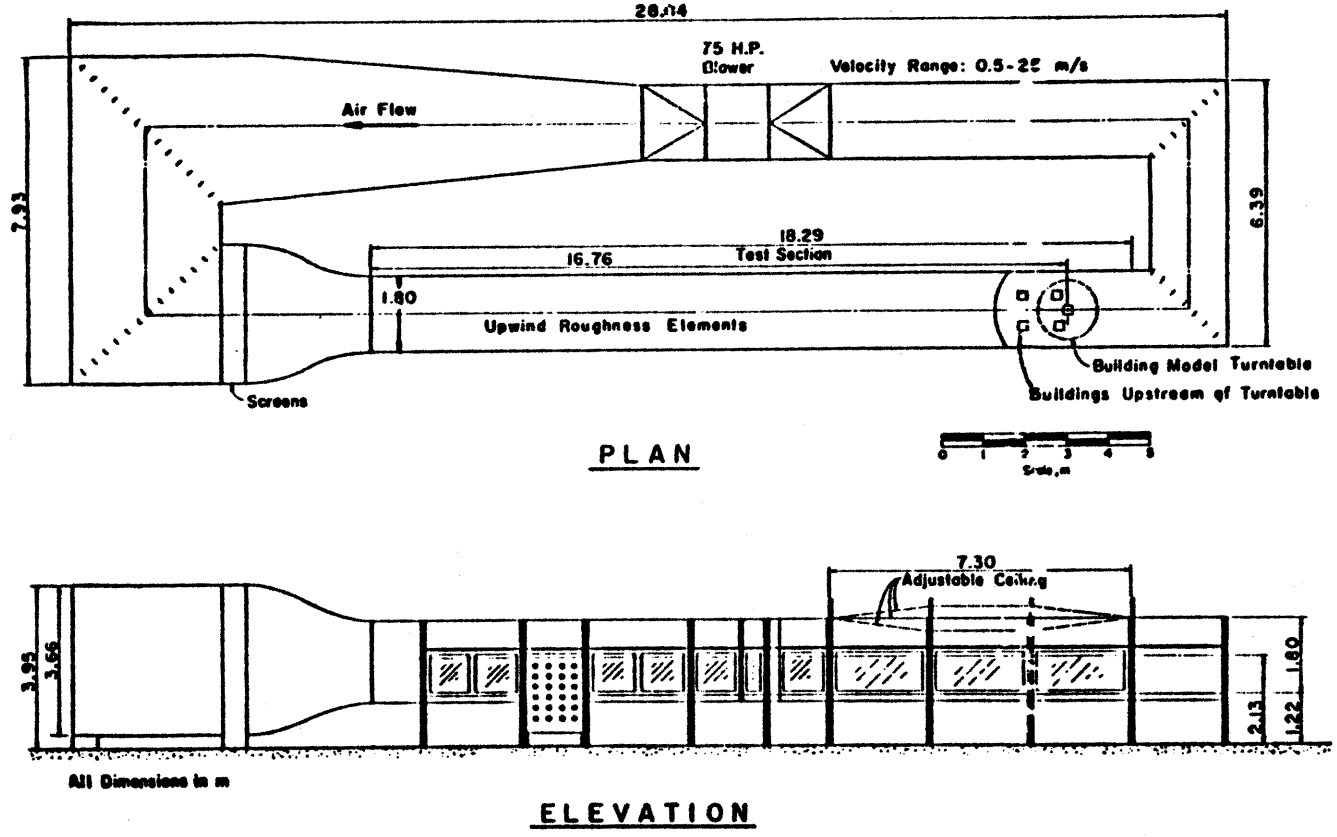

Figure 2. The Fluid Dynamics and Diffusion Laboratory Industrial Aerodynamics Wind Tunnel

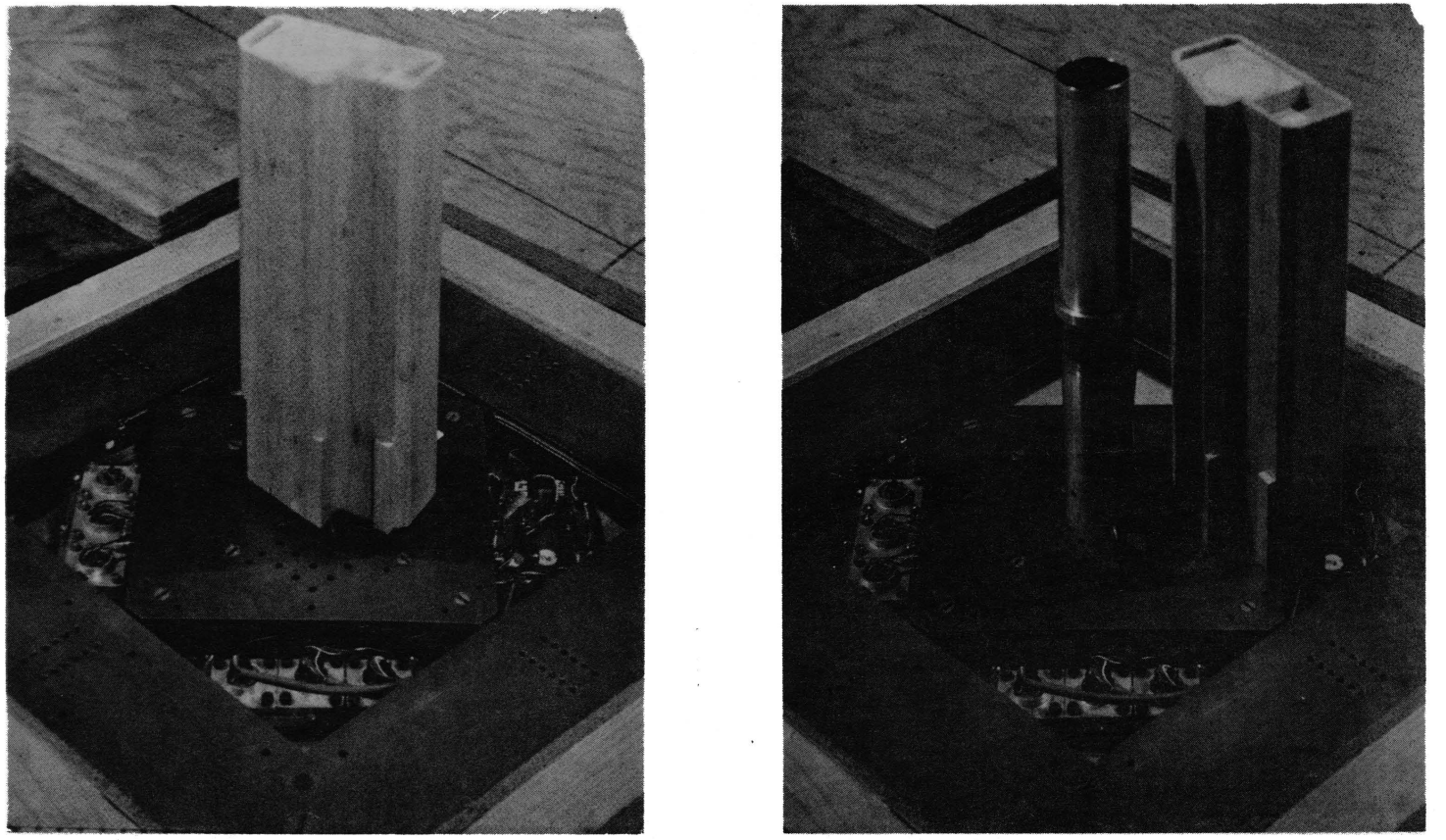

Figure 3. Model and Force Balance

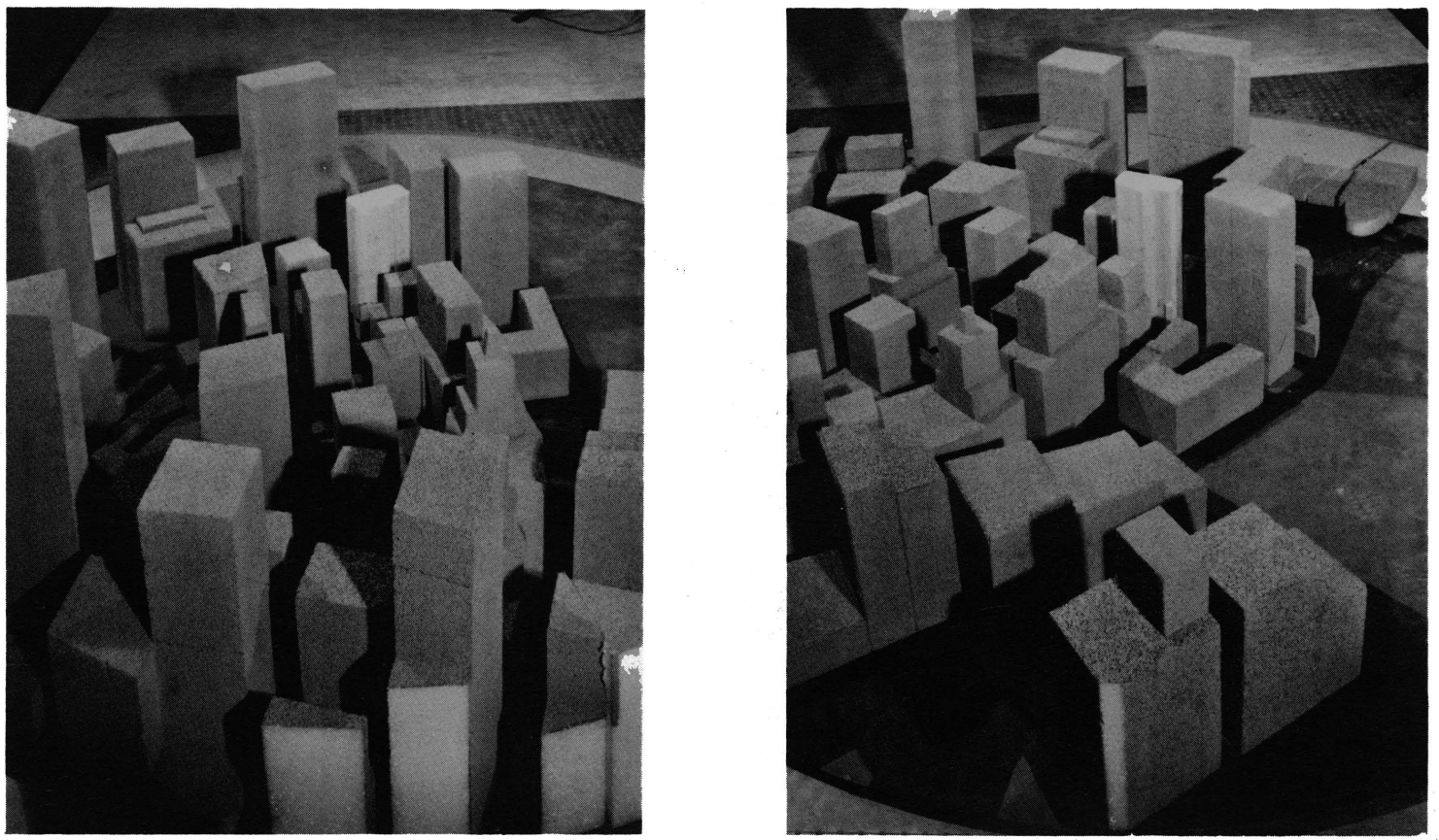

Figure 4. Model in City Environment

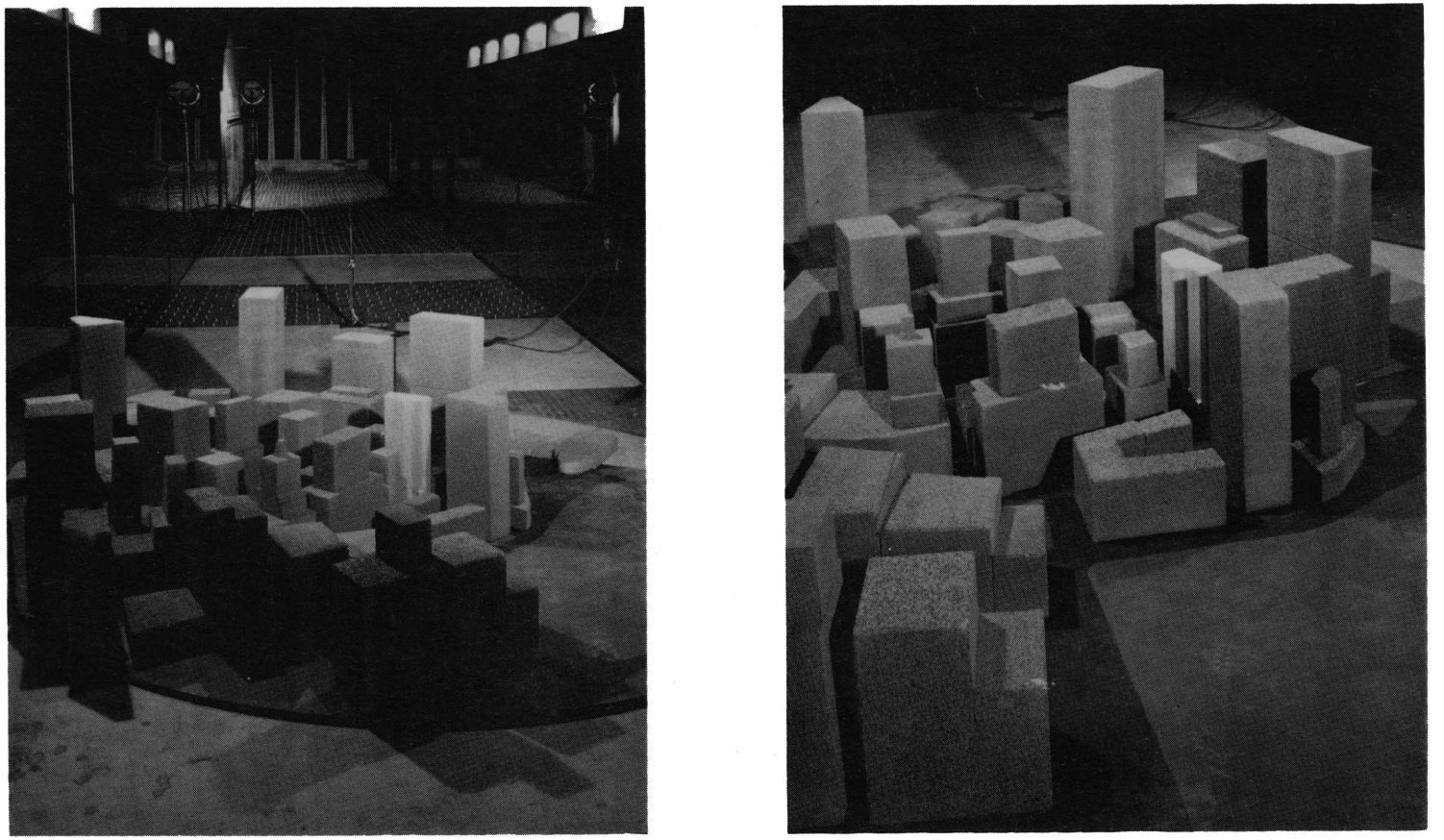

Figure 5. Model set up in the Wind Tunnel

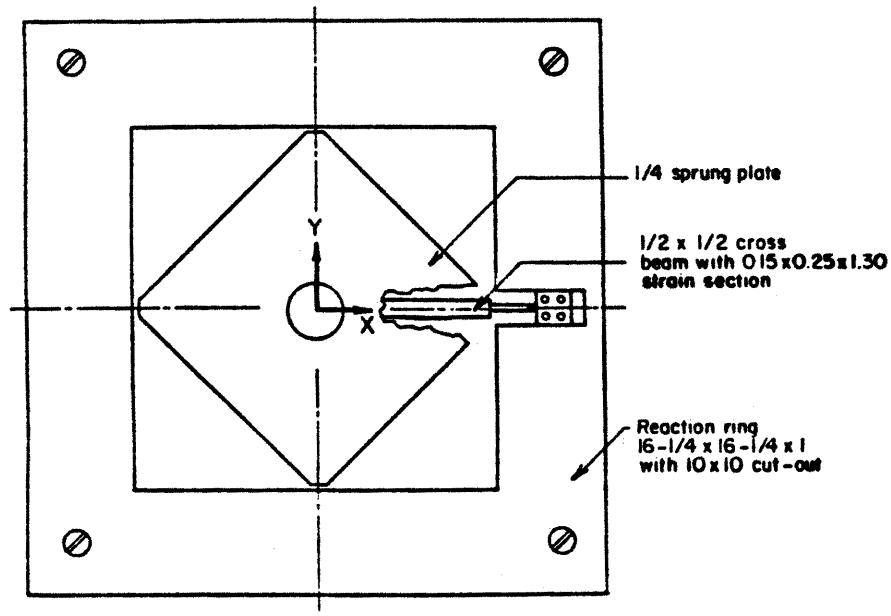

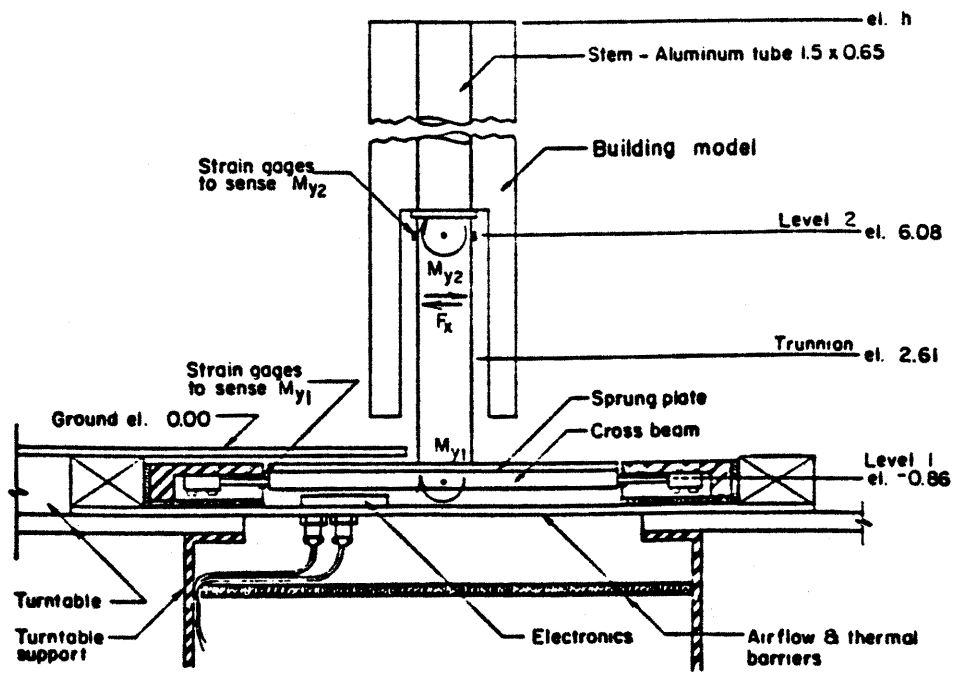

Figure 6. Schematic of Force Balance

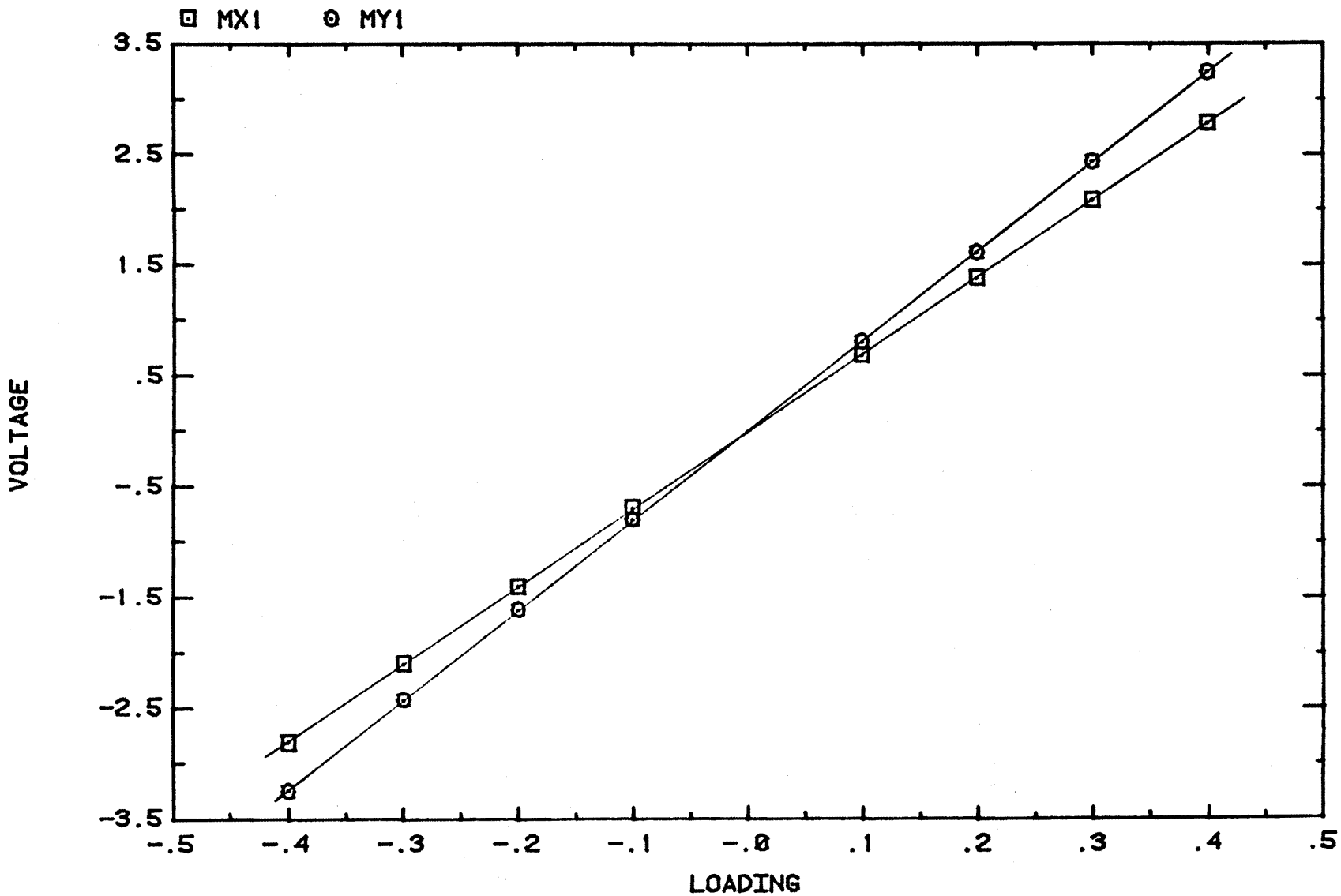

FIGURE 7. CALIBRATION CURVES

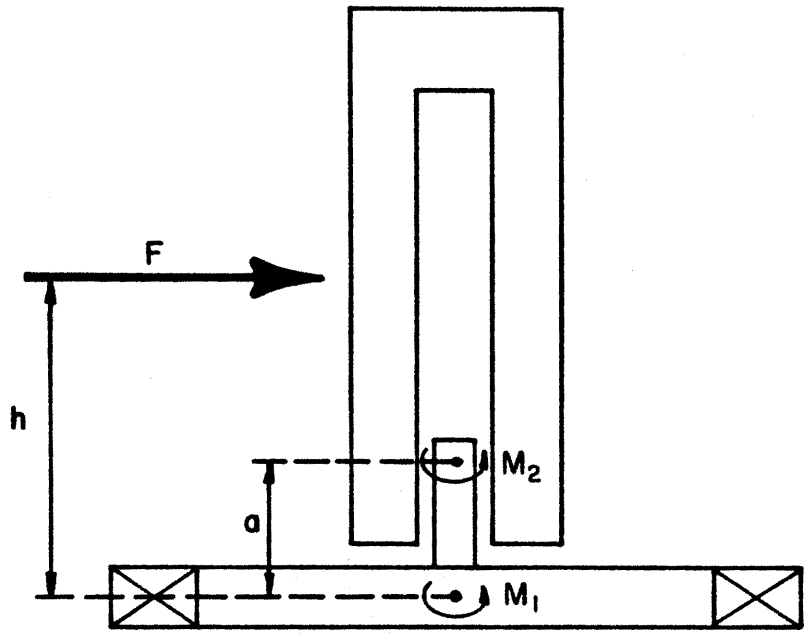

$$M_2 = -F(h-a)$$
$$M_1 = -F \cdot h$$

$$\Rightarrow \quad -M_2 + M_1 = -Fh + Fa + Fh = Fa$$
$$\Rightarrow \quad F = \frac{\Delta M}{a}$$

Figure 8. Calculation of Shear Forces

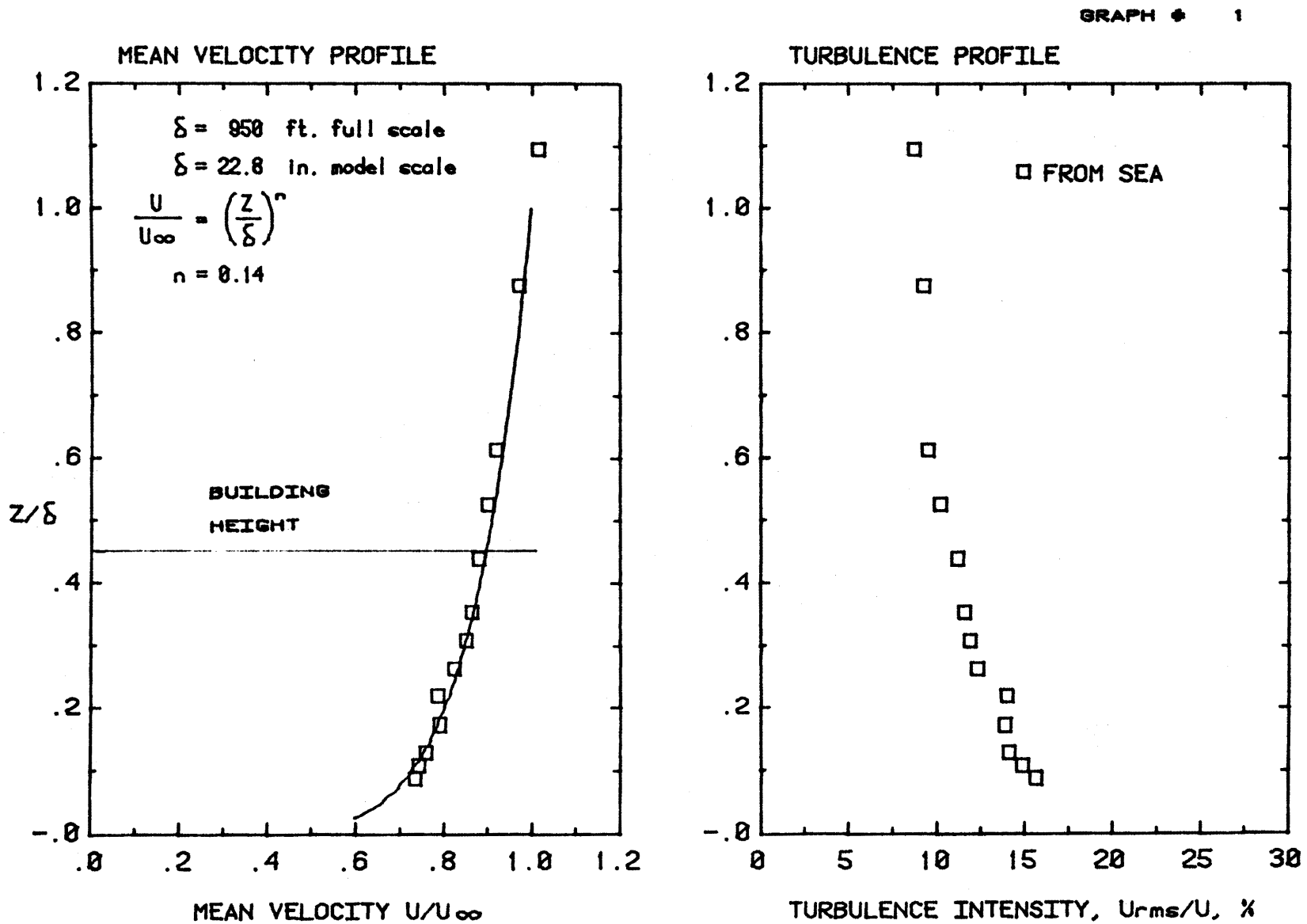

Figure 9. Mean Velocity and Turbulence Profiles Approaching the Model.

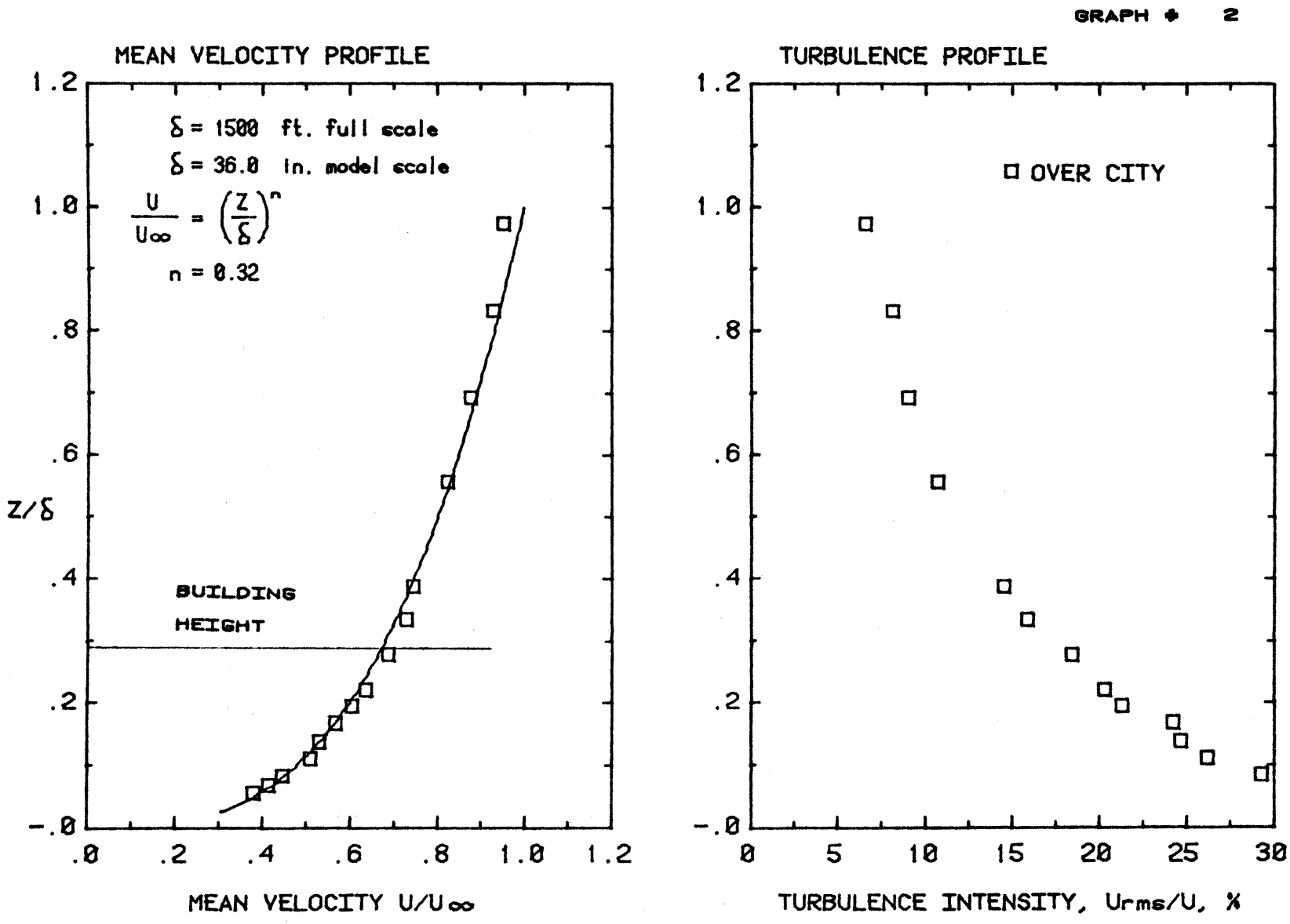

Figure 10. Mean Velocity and Turbulence Profiles Approaching the Model.

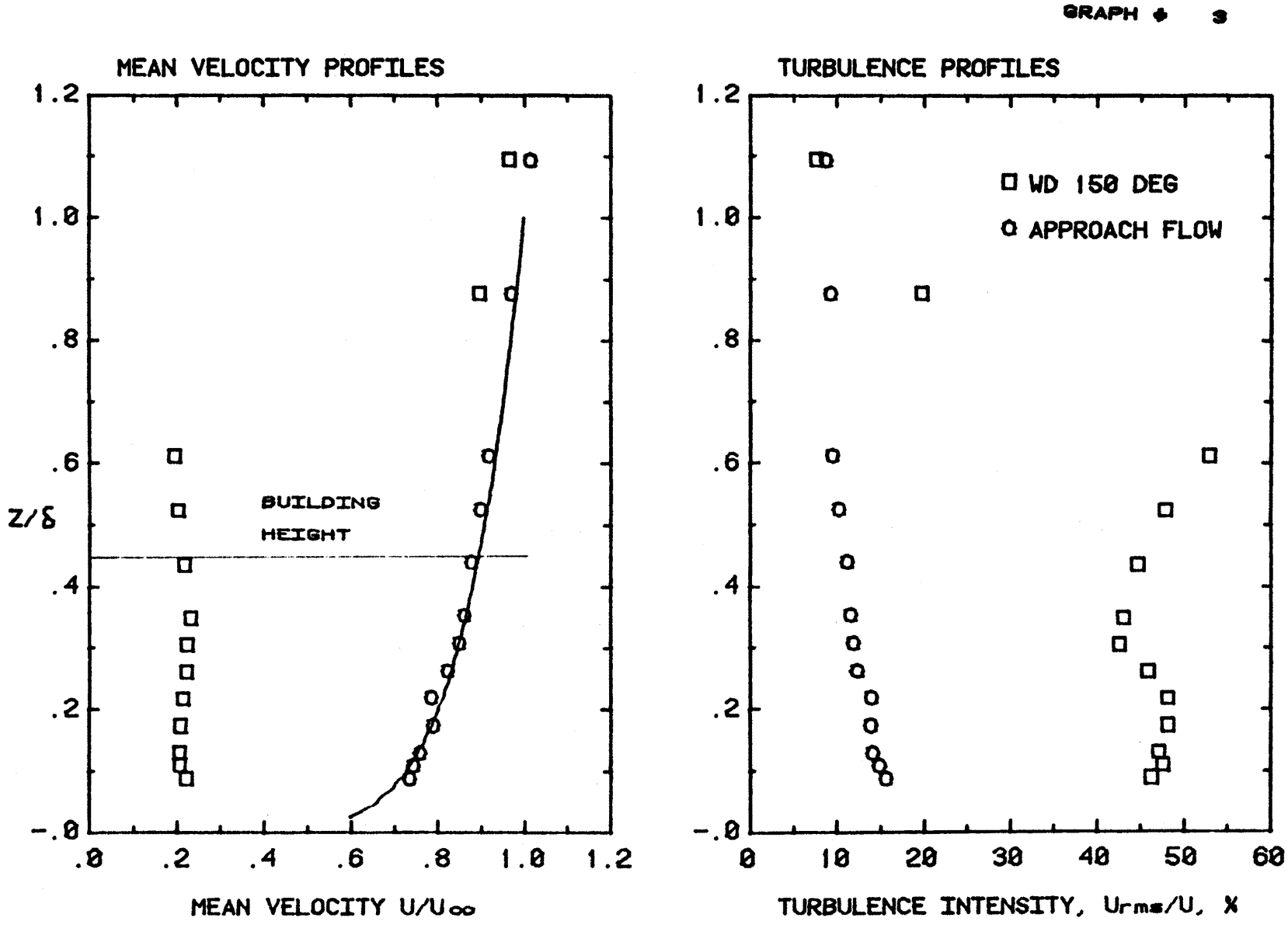

Figure 11. Mean Velocity and Turbulence Site Profile.

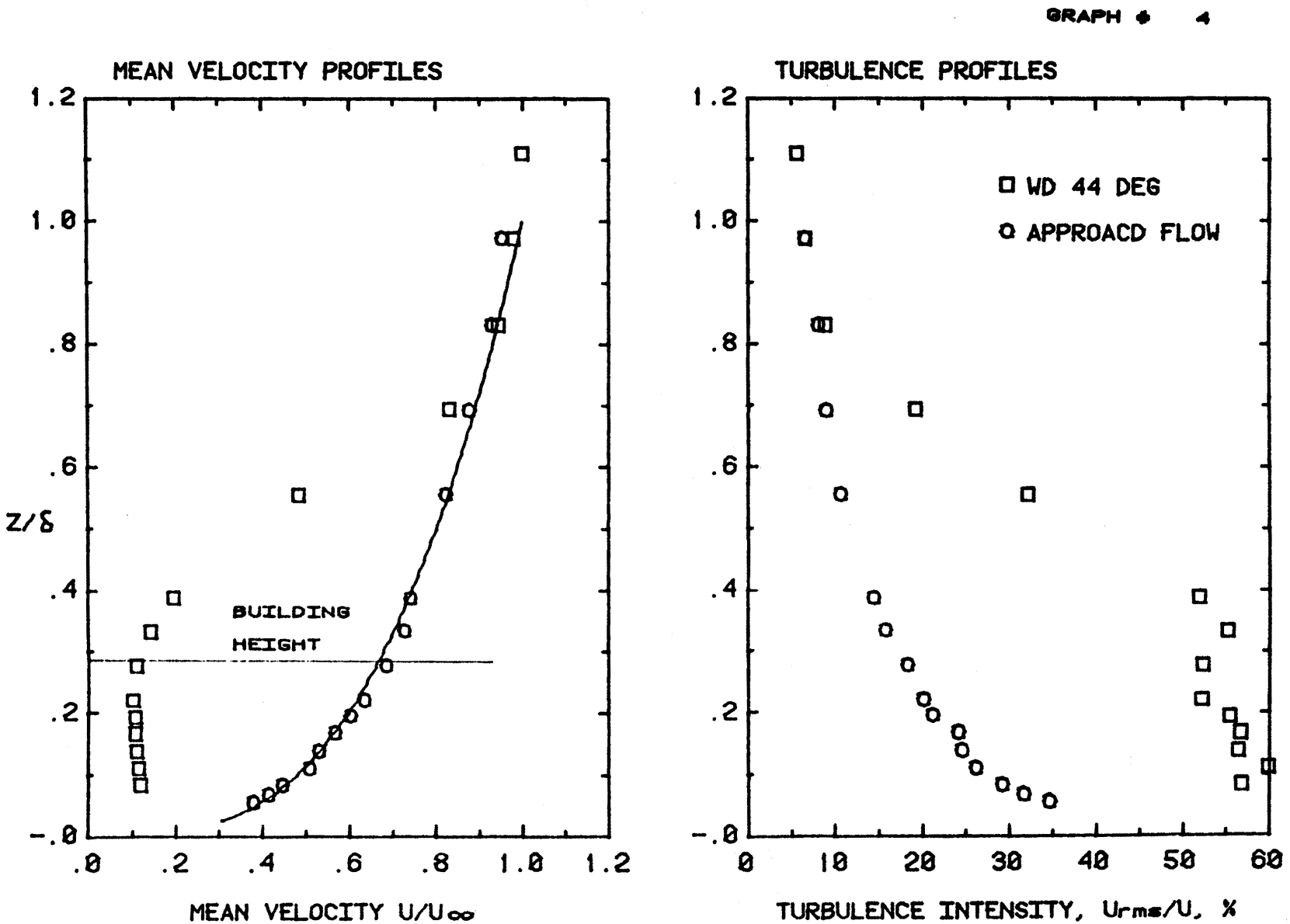

Figure 12. Mean Velocity and Turbulence Site Profile.

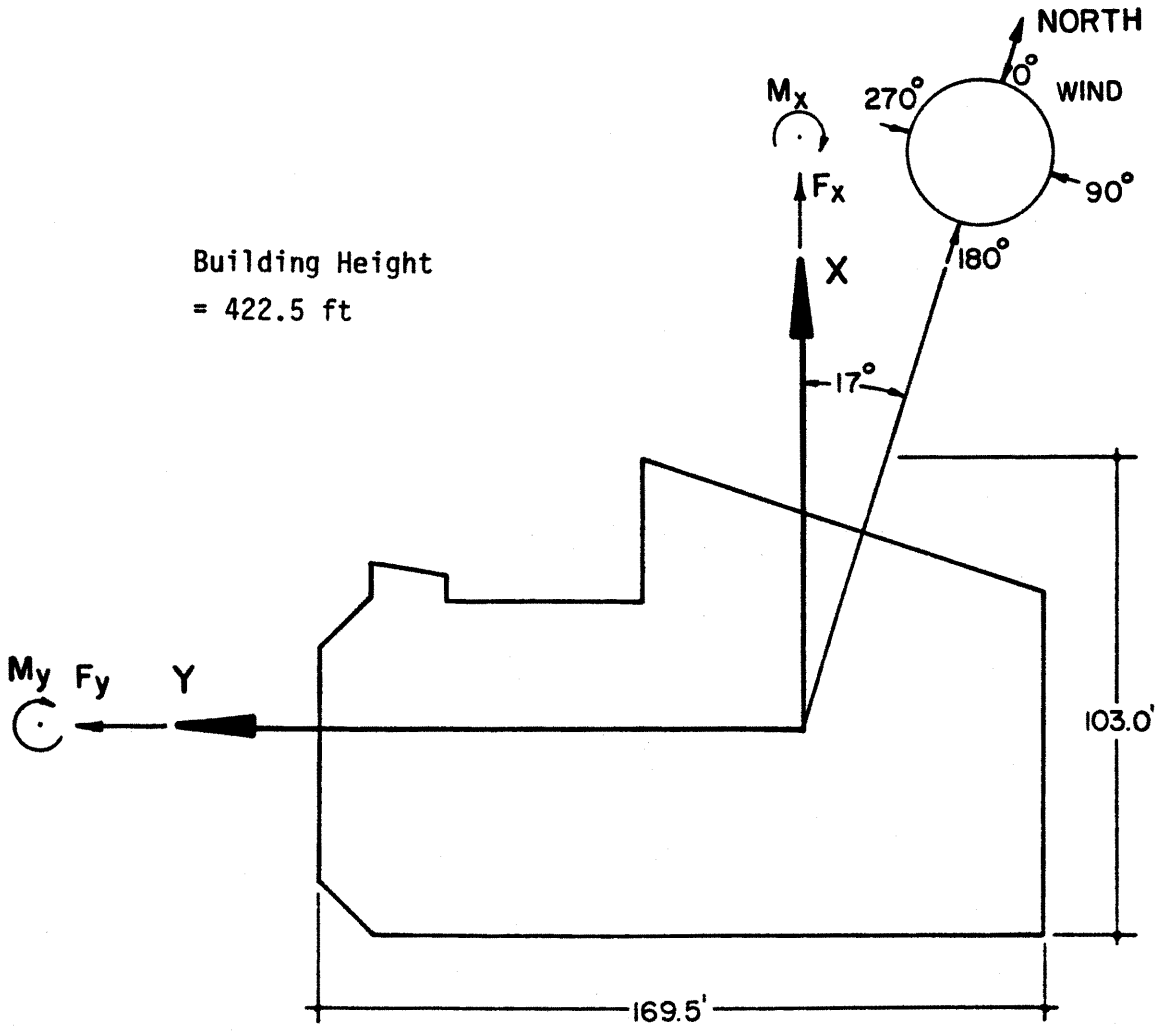

Figure 13. Force and Moment Coordinate System

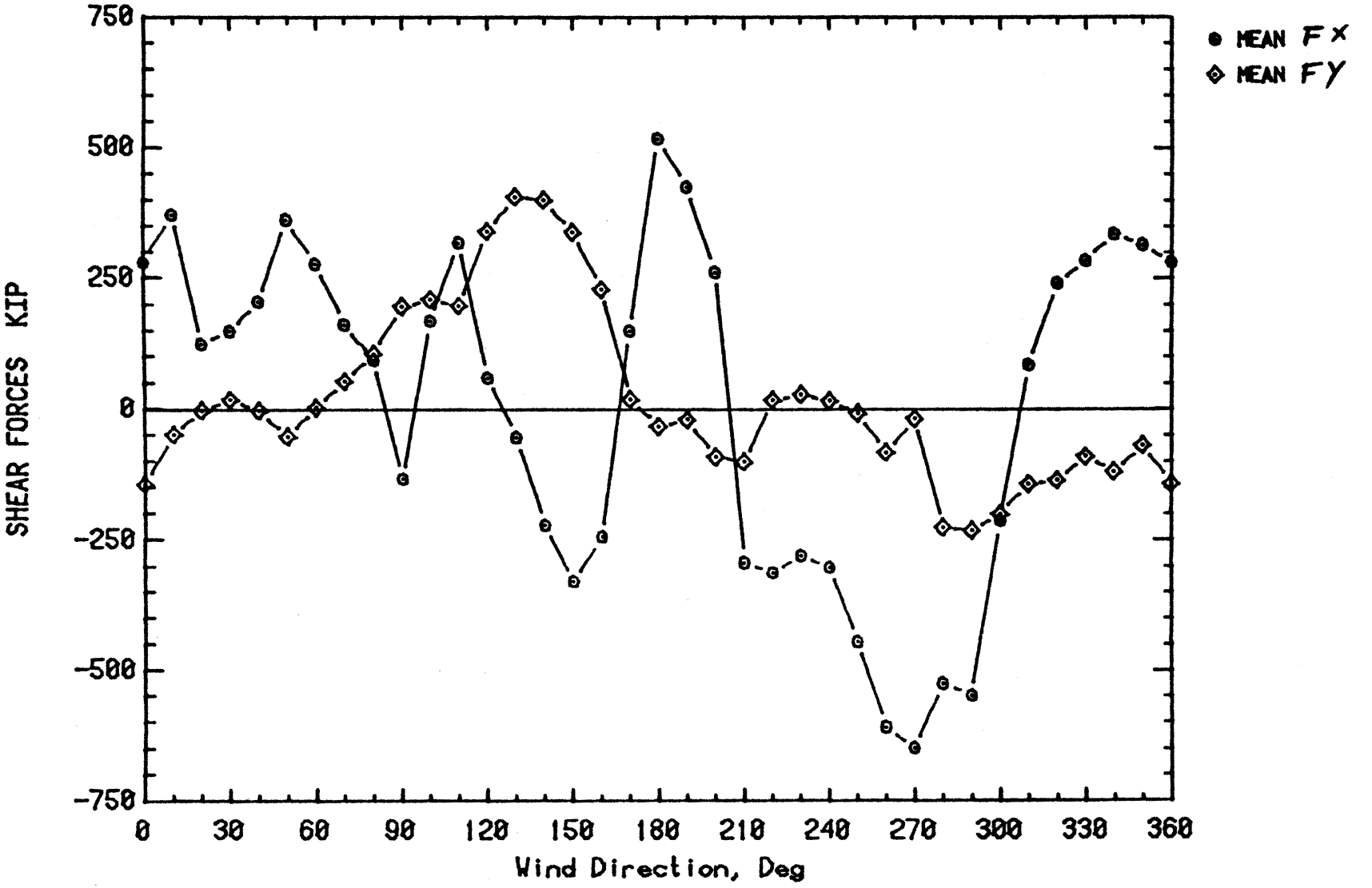

Figure 14. Moments

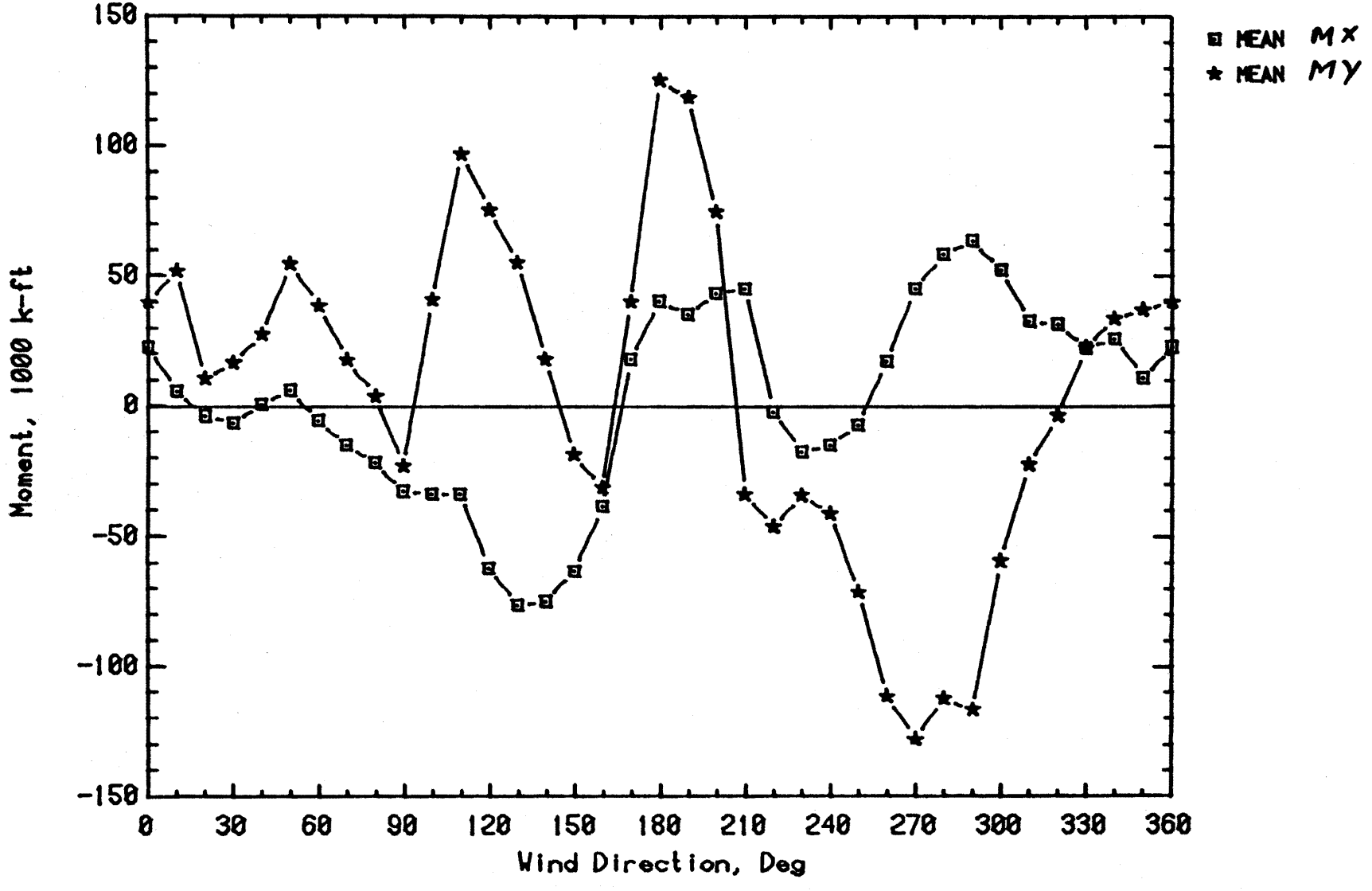

BROAD FINANCIAL CENTER, BUILDING IN CITY ENVIRONMENT

Figure 15. Shear Forces

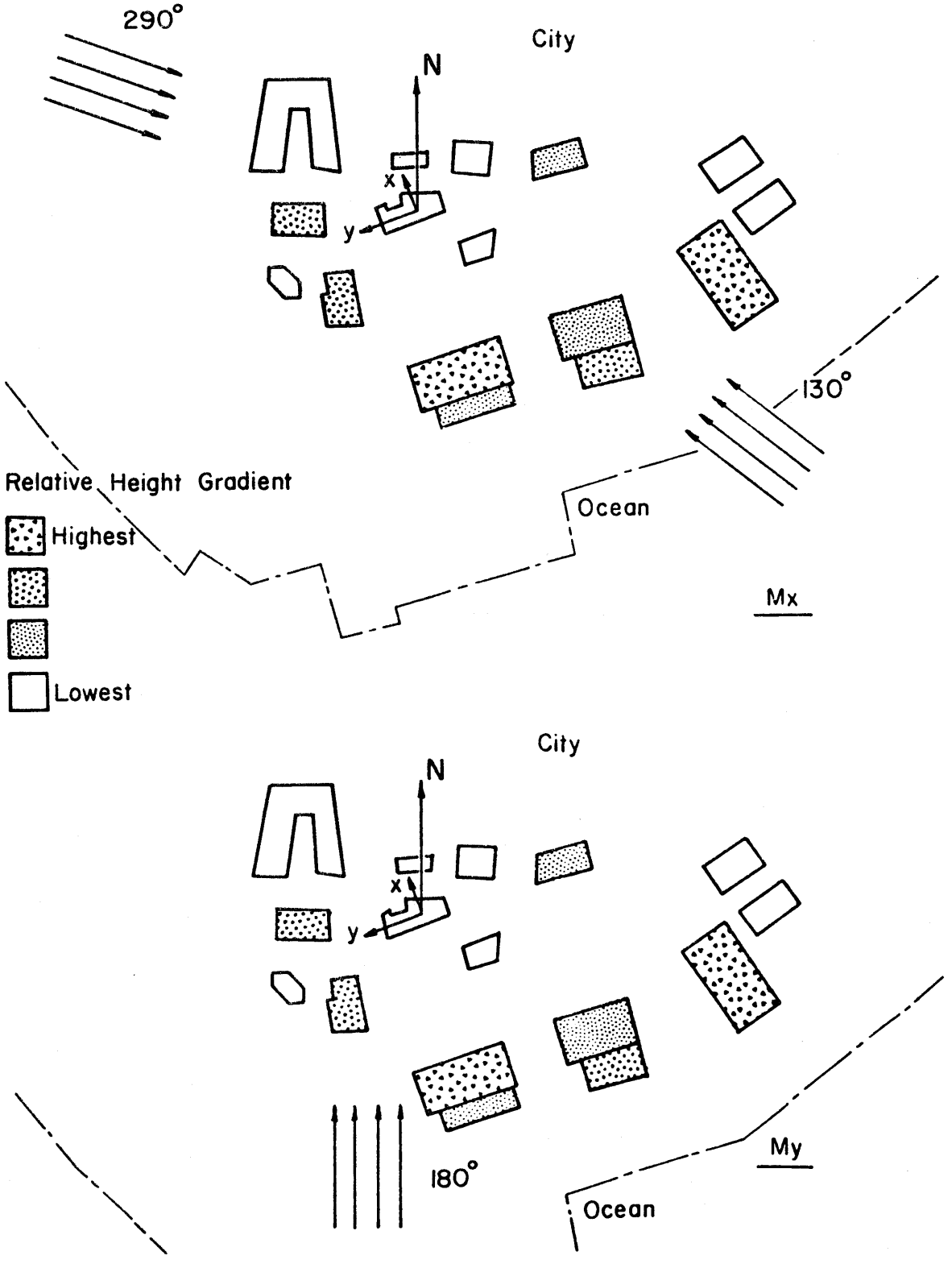

Figure 16. Wind directions and corresponding surroundings